U–Pb zircon ages (SHRIMP) for Cadomian and Early Ordovician magmatism in the Eastern Pyrenees: New insights into the pre-Variscan evolution of the northern Gondwana margin

Pedro Castiñeiras [a,b,*], Marina Navidad [b], Montserrat Liesa [c], Jordi Carreras [d], Josep M. Casas [e]

[a] Department of Geological Sciences, University of Colorado, Boulder, CO 80309-0399, USA
[b] Dpto. Petrología y Geoquímica-Instituto de Geología Económica (UCM-CSIC), Facultad de Ciencias Geológicas. Universidad Complutense, 28040 Madrid, Spain
[c] Dpt. Geoquímica, Petrologia i Prospecció Geològica. Universitat de Barcelona, Zona Universitària de Pedralbes, 08028 Barcelona, Spain
[d] Dpt. Geologia. Universitat Autònoma de Barcelona, 08193 Bellaterra (Cerdanyola del Vallès) Barcelona, Spain
[e] Dpt. Geodinàmica i Geofísica. Universitat de Barcelona, Zona Universitària de Pedralbes, 08028 Barcelona, Spain

A B S T R A C T

New geochronological data from low- to medium-grade metamorphic areas of the Eastern Pyrenees (Canigó, Roc de Frausa and Cap de Creus massifs) confirm the presence of two significant pre-Variscan igneous events: Ediacaran–Early Cambrian and Early Ordovician. The Ediacaran–Early Cambrian (580–540 Ma) magmatism is characterized by metavolcanic plagioclasic gneisses (metatuffs) coeval with sedimentation and by sheets of granitic orthogneisses emplaced in the lower part of the metasedimentary series. In the Canigó and Roc de Frausa massifs, the metatuffs are spatially associated with metabasites. Both lithologies occur as massive layers of lava flows, discontinuous lense-shaped, subvolcanic, gabbroic bodies or volcanoclastic tuffs interbedded in the lower and middle part of the pre-Upper Ordovician metasedimentary succession. This magmatism is bimodal and has a tholeiitic and calc-alkaline affinity. The granitic orthogneisses represent thick laminar intrusions of subaluminous and aluminous composition. Early Ordovician (475–460 Ma) magmatism is represented by laccoliths of aluminous granitic orthogneisses emplaced in the middle part of the pre-Upper Ordovician succession.

These geochronological data reveal the existence of an Ediacaran metasedimentary sequence and Cadomian magmatism in the Pyrenees and allow their correlation along the Eastern Pyrenean massifs. The data also show ages ranging from Neoproterozoic to Early Ordovician of the large bodies of granitic orthogneisses that intruded into the series at different levels. Both events represent the final stages of the Cadomian orogeny and its transition to the Variscan cycle in the Eastern Pyrenees. A Cambrian rifting event linking both cycles has not been identified in the Pyrenees to date.

Our findings provide a better fit for the pre-Variscan sequences of the Pyrenees with those of the Iberian Massif and allow their comparison with other pre-Variscan massifs in Europe.

Keywords:
Pre-Variscan
Cadomian
Ordovician magmatism
SHRIMP geochronology
U–Pb zircon dating
Eastern Pyrenees

1. Introduction

In recent years, the development of isotopic geochemistry and the improvement in geochronological methods have made great strides in the reconstruction of the Cadomian orogen and its geodynamic evolution and in the transition of the Cadomian to the Variscan cycle in the European realm (e.g., Stampfli et al., 2002; Linnemann et al., 2004; Samson et al., 2005; Gerdes and Zeh, 2006). In this regard, the Iberian Massif has played a major role for three main reasons: (i) good preservation of pre-Variscan sediments, unaffected or affected by very low grade metamorphism, (ii) fairly complete stratigraphic sequences with thick Precambrian series, and (iii) the presence of volcanic and plutonic rocks emplaced in several stratigraphic levels at different times and with diverse geochemical signatures (Nägler et al., 1995; Fernández-Suárez et al., 1998; Valladares et al., 2002; Bandrés et al., 2004; Rodríguez-Alonso et al., 2004; Silva and Pereira, 2004; Díaz García, 2006 and references therein).

In the Pyrenees, the presence of an important Early Ordovician magmatic event (Delaperrière and Respaut, 1995; Deloule et al., 2002; Cocherie et al., 2005) and its relationship with the lower levels of the pre-Upper Ordovician metasedimentary sequence have led some authors to rule out the existence of Cadomian magmatism (e.g., Laumonier et al., 2004). Recently, Cocherie et al. (2005) obtained an Ediacaran age for a metatuff from the lower levels of the sequence. Nevertheless, the age of the upper part of the metasedimentary

* Corresponding author. Dpto. Petrología y Geoquímica-Instituto de Geología Económica (UCM-CSIC), Facultad de Ciencias Geológicas. Universidad Complutense, 28040 Madrid, Spain. Tel.: +34 91 3944898; fax: +34 91 5442535.
E-mail address: castigar@geo.ucm.es (P. Castiñeiras).

sequence and the location of the Ediacaran–Cambrian boundary is still a matter of debate because of its unfossiliferous character.

We present new geochronological data obtained from six samples of three Eastern Pyrenean massifs in an attempt to gain further insight into the Cadomian orogen, its transition to the Variscan orogen, and on the controversy over the importance of the Cadomian signature in the Pyrenees. From west to east, these massifs are (Fig. 1): Canigó (known as Canigou in the French literature), Roc de Frausa (also known as Roc de France) and Cap de Creus. The new data confirm the existence of an Ediacaran–Lower Cambrian metasedimentary sequence with coeval volcanism in the Pyrenean pre-Variscan massifs. We also obtained Cadomian and Ordovician ages for orthogneisses emplaced at different structural levels in these metasediments. Inherited ages and detrital zircons analyzed in the volcanic and volcano-sedimentary samples provide some insights into the sources of these rocks and their correlation with other pre-Variscan complexes. The geological data obtained from several areas enable us to the characterize the Cadomian orogenic stages (collision, arc magmatism and breakup and amalgamation of the peri-Gondwanan basins) along the northern margin of Gondwana, and to understand the evolution of the Variscan cycle with the opening and closure of the Rheic Ocean (von Raumer et al., 2002; Stampfli et al., 2002; Murphy et al., 2004).

2. Geological setting

In the Pyrenees, Alpine tectonics has exposed an extensive E–W trending area, the so-called Axial Zone, where a thick pre-Variscan succession crops out in several massifs (Fig. 1).

The lower part of this succession is a thick azoic metasedimentary sequence (Fig. 2), pre-Upper Ordovician in age, locally cut by orthogneiss sheets near the base of the sequence (Cavet, 1957). This author described a heterogeneous sequence at the base made up of metapelites and metagreywackes with interbedded metavolcanic rocks. At the top, the sequence consists of a monotonous succession of shales, sandstones and quartzites. Laumonier (1988) established a more detailed subdivision of the sequence based on lithological criteria.

A well-dated Upper Ordovician succession, with Caradocian conglomerates (Cavet, 1957; Hartevelt, 1970) generally at the base, lies unconformably over the former metasediments (Santanach, 1972b; Casas and Fernández, 2007). The absence of a biostratigraphic control in the pre-Upper Ordovician sequence makes the evaluation of the magnitude of this unconformity difficult. Nevertheless, it has been suggested that at least the Lower and Middle Ordovician sediments were removed before deposition of the Upper Ordovician rocks (Muñoz and Casas, 1996). Silurian and Devonian strata, consisting respectively of siliciclastic sediments and limestones, follow in stratigraphic continuity. On top of the series, black shales, cherts and limestones constitute a Carboniferous pre-orogenic sequence.

The whole succession was affected by Variscan deformation (late Visean to Serpukhovian) accompanied by high temperature–low pressure metamorphism (Guitard, 1970; Zwart, 1979). Syn- to late orogenic (Moscovian–Kasimovian) granitoids intruded mainly into the upper levels of the succession, producing local contact metamorphism (Autran et al., 1970).

The pre-Upper Ordovician sequences are well developed in the Eastern Pyrenees, whereas in the Central Pyrenees thick Devonian and Carboniferous series are predominant. In the studied massifs (Canigó, Roc de Frausa and Cap de Creus), the pre-Upper Ordovician sequence is mainly composed of a metapelitic series sporadically interbedded with numerous layers of metabasites, rhyodacitic tuffs, marbles, quartzites and calc-silicates. The orthogneisses are variably thick, from ~2 km (at the Canigó massif) to 100 m (at the Cap the Creus massif).

2.1. Canigó massif

This massif exhibits the most complete pre-Upper Ordovician metasedimentary succession of the Eastern Pyrenees (Fig. 2). The succession can be divided into three series (Cavet, 1957). The lowermost part

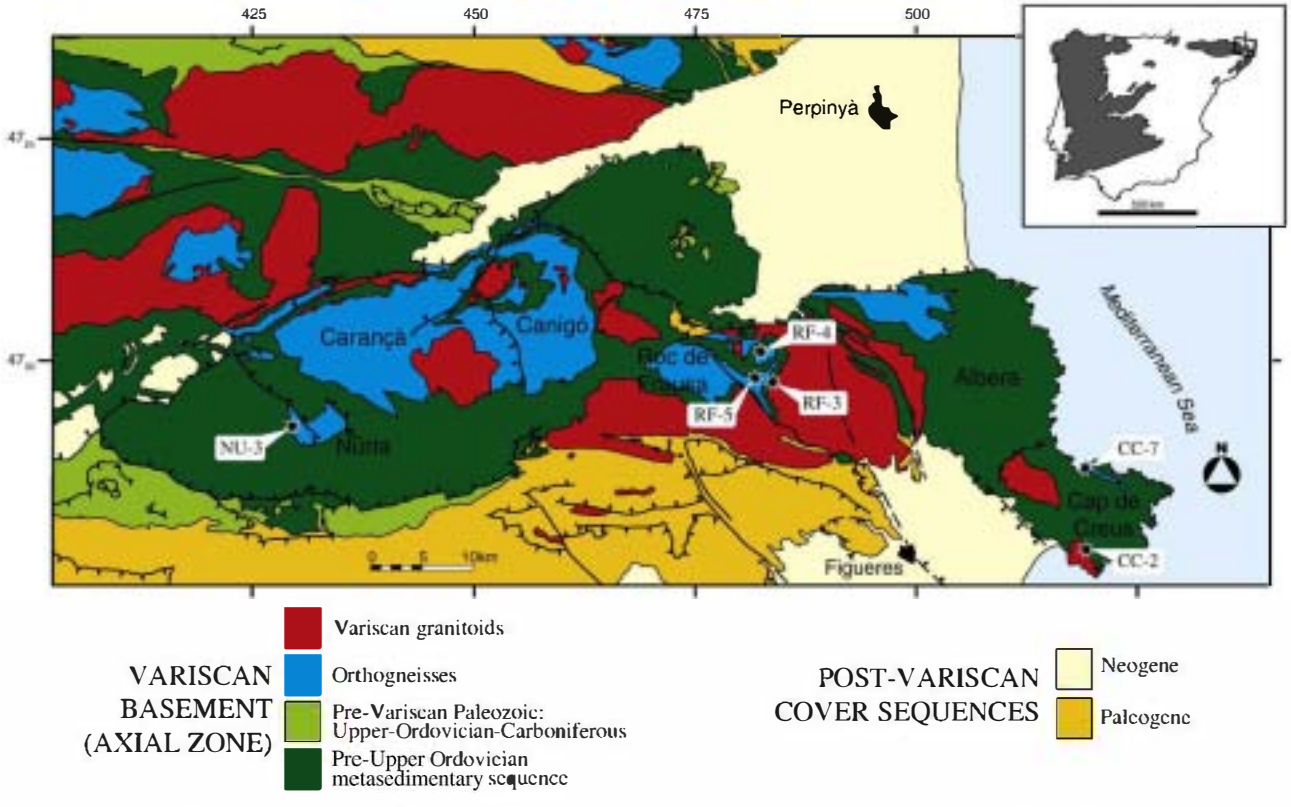

Fig. 1. Geological sketch of the Variscan basement of the Eastern Pyrenees and cover sequences with location of the stratigraphic columns and the studied samples.

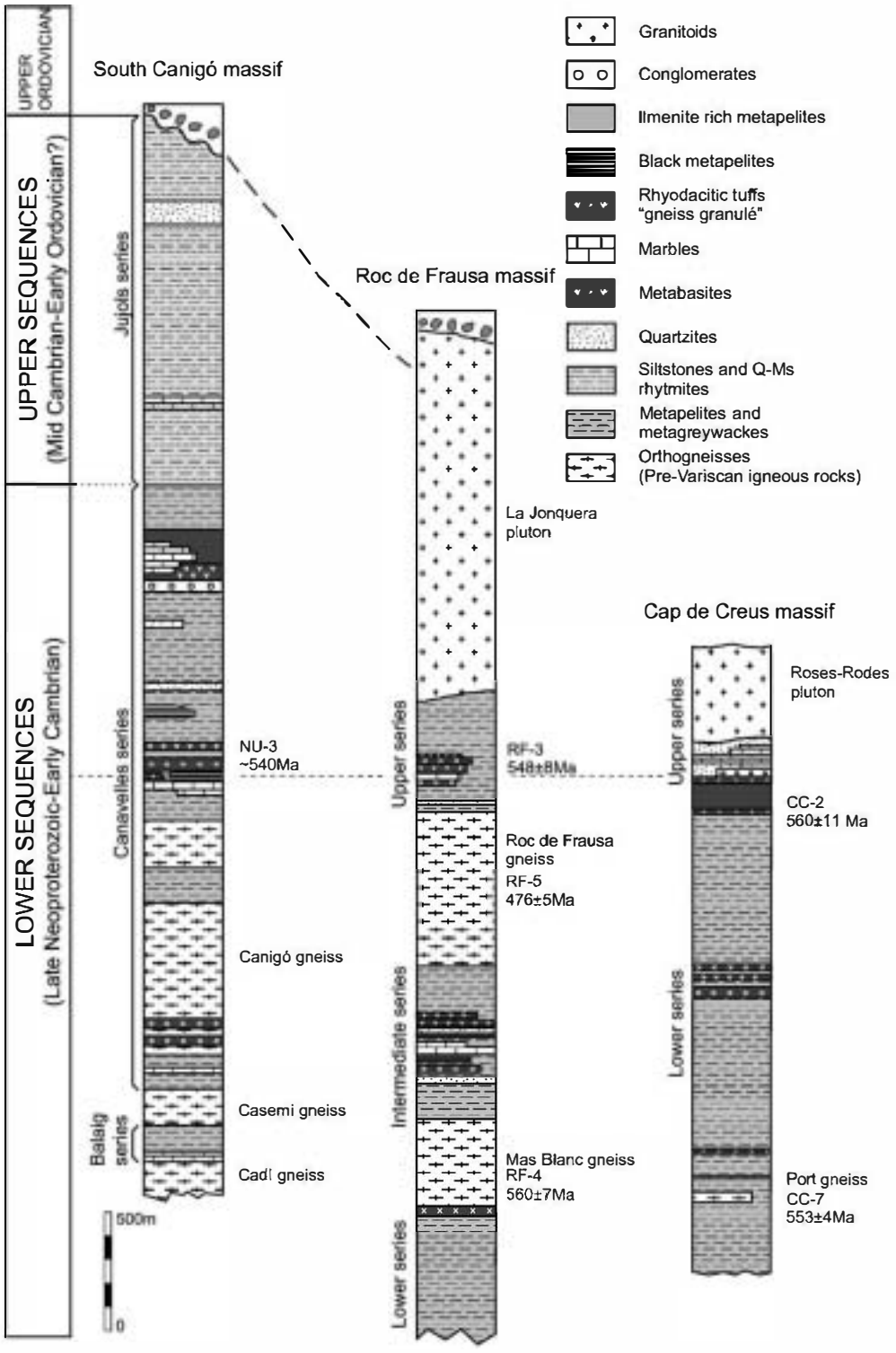

Fig. 2. Synthetic stratigraphic columns of the pre-Upper Ordovician rocks of the Canigó, Roc de Frausa and Cap de Creus massifs with the location of the studied samples. Data compiled from Guitard (1970), Santanach (1972a) and Ayora and Casas (1986) for the Canigó massif; Liesa and Carreras (1989) for the Roc de Frausa massif and Carreras et al. (1994), and Losantos et al. (1997) for the Cap de Creus massif.

consists of a thick sequence, the Balaig micaschists, made up of biotite-rich micaschists with interlayered marbles, metabasites and quartzites (Guitard, 1970). The intermediate part is formed by the Canavelles Series (the Canaveilles Series of Cavet, 1957), a heterogeneous sequence mainly composed of alternating metagreywackes and metapelites interbedded with numerous layers of marbles, quartzites, ilmenite-rich micaschists, black phyllites, calc-silicates and a variety of metavolcanic rocks (Cavet, 1957; Guitard, 1970; Casas et al., 1986; Ayora and Casas, 1986). At the top, the Jujols Series consists of a monotonous rhythmic sequence composed of shales, sandstones and quartzites (Cavet, 1957).

In addition, three different granitic orthogneissic bodies are located in the basal levels of the pre-Upper Ordovician sequence (Fig. 1). The Cadí gneiss (Guitard, 1970) constitutes the deepest rock outcropping in this area below the Balaig micaschist. The Casemí gneiss (Guitard, 1970; Delaperrière and Soliva, 1992) is a leucocratic, fine-grained orthogneiss interlayered into the Balaig micaschist. Finally,

the Canigó gneiss separates the Balaig micaschist from the Canavelles Series. This gneiss is formed by thick (more than 2000 m) stratoid porphyritic granitic gneisses (Guitard, 1970).

Pre-Variscan volcanic rocks are frequent in the Canavelles Series. They are made up of basaltic andesites (transformed to metabasites) and of rhyolithic and rhyodacitic tuffs (transformed to metatuffs), commonly known as *gneiss granulé* by French geologists (Guitard and Laffitte, 1956; Guitard, 1970). Decametre-scale layers of metabasites consisting of amphibole, plagioclase and ilmenite are widely present on the eastern and southern slopes of the massif (Guitard, 1970; Casas et al., 1986; Navidad and Carreras, 2002). They correspond to calc-alkaline and ocean floor back-arc tholeiites and are spatially linked to 2–4 m thick layers of metarhyolithic and metarhyodacitic pyroclasts (Ayora and Casas, 1986; Navidad and Carreras, 2002). Metatuffs have a calc-alkaline affinity and are related to an explosivevolcanism (Navidad and Carreras, 2002). They are well developed in the southern slope of the massif, where they form a thick level (up to 200 m) in the upper part of the Canavelles Series, giving rise laterally to conglomerates, black shales, limestones and feldspathic sandstones (Fig. 2). Field relationships suggest that this bimodal volcanism is coeval. This can be related to either a back-arc or a marginal continental basin along the northern Gondwana margin (Navidad and Carreras, 1995, 2002; Navidad et al., 1996).

A representative metatuff interbedded in the lower part of the Canavelles Series was collected from the southeastern Canigó massif, in the Núria area near Queralbs (sample NU-3, Fig. 1). This sample presents characteristics similar to those of another metatuff collected 20 km further east, in the central part of the Canigó massif, dated at 581 Ma (U–Pb SHRIMP method in zircon, Cocherie et al., 2005).It was sampled to confirm the age of the Canavelles Series in the southeastern part of the Canigó massif owing to the uncertainity of the detailed stratigraphic position of sample GRA-1. A representative sample of the mafic volcanism was also collected but it yielded no zircon.

2.2. Roc de Frausa massif

In this massif, the top of the pre-Upper Ordovician sequence is masked by the intrusion of the Variscan La Jonquera pluton (Fig. 2). Additionally, two thick gneissic bodies, the Mas Blanc and the Roc de Frausa orthogneisses (Autran and Guitard, 1969), divide the sequence into three series (Fig. 2). The lower series is lithologically monotonous and formed by coarse-grained metagreywackes with scarce amphibolite layers intercalated. Even though its correlation is unclear, it could be equivalent to the Balaig michaschist of the neighbouring Canigó massif. The intermediate and upper series are formed by reddish coarse-grained metagreywackes alternating with ~100 m thick packs of lighter-colored quartzose metapelites and metagreywackes. In turn, the metapelites are interbedded with layers of varied lithologies: amphibolites, metatuffs, marbles, calc-silicates, quartzites and black pelites, giving rise to a lithologically complex unit. Among the metasediments, marble is the most important lithology, cropping out as layers up to 50 m thick. This metasedimentary sequence can be correlated with the Canavelles Series defined in the Canigó massif (Liesa and Carreras, 1989).

Metabasites are spatially related to gneissic porphyroids (metatuffs). The metabasites form thin and usually discontinuous layers along the sequence and the volcanic protoliths are tholeiitic basalts or basaltic andesites (Navidad et al., 1996). The metatuffs form metre-scale discontinuous layers consisting of milimetre-sized plagioclase porphyroclasts in a foliated matrix. Their protoliths are subalkaline rhyodacitic tuffs and rhyolites (Navidad et al., 1996).

The Mas Blanc and the Roc de Frausa orthogneisses are coarse-grained aluminous augengneisses with microcline porphyroclasts. Isotopic data reveal a crustal origin for these rocks (Liesa and Carreras, 1989). Contacts of the gneisses with the metasediments are generally sharp and, in the Roc de Frausa gneiss, small apophyses can be found in the metasediments. Near the contact, the Roc de Frausa gneisses are fine-grained and lack porphyroclasts, while the Mas Blanc gneisses are always coarse-grained. The Mas Blanc gneiss is richer in biotite and the plagioclase in more calcic than of the Roc de Frausa gneiss.

Sample RF-3 is a metatuff collected to date the upper series of the metasedimentary sequence in the Roc de Frausa massif (Fig. 2). Sample RF-4 corresponds to the Mas Blanc orthogneiss, and sample RF-5 was collected from the Roc de Frausa orthogneiss (Fig. 2).

2.3. Cap de Creus massif

In this massif, the pre-Upper Ordovician sequence can be divided into two series according to the lithologies. The lower series is an 800 m thick monotonous alternance of predominant greywackes, subordinate pelites and discontinuous layers of plagio-amphibolites. Banded quartzites form distinct continuous layers ranging in thickness from a few centimeters to a few meters. This sequence is overlain by a sequence of carbonaceous black slates interbedded with marbles and acidic metaporphyries. The upper series is mainly formed by conglomerates, siliciclastic sediments and carbonates with marked lateral changes (Carreras et al., 1994). Granitic orthogneisses (known as Port gneisses, Carreras and Ramírez, 1984) and metabasites crop out at the bottom and mid part of the lower sequence, whereas metatuffs are interstratified at the top. The protolith of the Port gneiss is a small intrusion derived from subalkaline granites to quartz-monzonites composed of scarce K-feldspar megacrysts in a fine-grained matrix. Metabasites comprise gabbrodoleritic intrusions and metabasaltic lens-shaped bodies. Minor element geochemistry indicates that they are low-K tholeiites (Navidad and Carreras, 1995).

The metatuffs contain feldspar and quartz porphyroclasts in a fine-grained matrix. They correspond to Al-rich calc-alkaline rhyolites and rhyodacites (Navidad and Carreras, 1995).

Five samples from the Cap de Creus were selected for U–Pb zircon analysis, including the Port gneiss (sample CC-7), metabasites (samples CC-4 to CC-6) and a metatuff (sample CC-2), in order to ascertain the age of the bimodal magmatism from this massif but again, there was no zircon yield from the metabasites.

3. Geochronological background

The age of the pre-Upper Ordovician metasediments and the granitic orthogneisses in the pre-Variscan massifs of the Pyrenees has been a matter of debate since the work of Fontboté (1949), Cavet (1957) and Guitard (1970). Initial studies (see Table 1) concluded that large granitic orthogneisses were situated at the core of metamorphic massifs, representing a Cadomian basement overlain by a lower Paleozoic cover (Autran and Guitard, 1969; Guitard, 1970; Vitrac-Michard and Allègre, 1975). In contrast, pioneering geochronological work in the Central Pyrenees pointed to an Ordovician age for the orthogneisses (see Table 1, Jäger and Zwart, 1968; Majoor, 1988). The advances made in U–Pb geochronology have revealed that some of the granitic orthogneisses are Early Ordovician in age. These granites intruded into a pre-Upper Ordovician metasedimentary sequence, thus invalidating the basement-cover model (Deloule et al., 2002; Cocherie et al., 2005). The implications of the nonexistence of a Cadomian granitic basement and the presence of an Ordovician magmatism in the Eastern Pyrenees (comparable to the one described in other areas of northern Gondwana; Pin and Marini, 1993; Santos Zalduegui et al., 1995; Valverde-Vaquero and Dunning, 2000) have been extensively discussed in subsequent alternative interpretations (e.g., Autran and Guitard, 1996; Barbey et al., 2001; Deloule et al., 2002; Laumonier et al., 2004; Cocherie et al., 2005).

The exact age of the pre-Upper Ordovician metasediments has also been a matter of debate due to their azoic character. According to its stratigraphic position, this sequence has been termed pre-Caradocian (Fontboté, 1949) or Cambro–Ordovician (Cavet, 1957) and it has been correlated with the Cambrian and Ordovician successions of the southern slopes of the Montagne Noire. High-grade paragneisses located in the lowermost part of the pre-Upper Ordovician sequences

Table 1
Available geochronology in the pre-Variscan massif of the Pyrenees

Massif	Lithology	Age	Method	Reference
Central Pyrenees				
Aston	Augengneiss	475	Rb/Sr isochron	1
Hospitalet	Leucogneiss	470	Rb/Sr	2
Sant Barthelemy	Sil orthogneiss	506±12	Single zircon evaporation	3
Sant Barthelemy	Milonitic granodiorite	526±7	Single zircon evaporation	3
Sant Barthelemy	Paragneiss	539±26	Rb/Sr isochron	4
Eastern Pyrenees				
Agly	Paragneiss	~550	Rb/Sr	5
Canigó	Augengneiss (G2-type)	580±20	U–Pb TIMS	5
Canigó	Augengneiss (G2-type)	451±14	Single zircon evaporation	6
Canigó	Núria orthogneiss (G1-type)	570±12	Single zircon evaporation	6
Canigó	Núria orthogneiss (G1-type)	461±7	Single zircon evaporation	6
Canigó	La Preste orthogneiss (G1-type)	446±20	Single zircon evaporation	7
Canigó	Augengneiss	475±10	U–Pb SIMS	8
Casemi	Leucogneiss	425±18	Single zircon evaporation	9
Canigó	Orthogneiss	477±4	U–Pb SHRIMP	10
Canigó	Orthogneiss	472±6	U–Pb SHRIMP	10
Canigó	Orthogneiss	471±8	U–Pb SHRIMP	10
Canigó	Orthogneiss	467±7	U–Pb SHRIMP	10
Canigó	Metarhyodacite (GRA-1)	581±10	U–Pb SHRIMP	10

1: Jäger and Zwart (1968); 2: Majoor (1988); 3: Delaperrière et al. (1994); 4: Marshall (1987); 5: Vitrac-Michard and Allègre (1975); 6: Guitard et al. (1996); 7: Delaperrière and Respaut (1995); 8: Deloule et al. (2002); 9: Delaperrière and Soliva (1992); 10: Cocherie et al. (2005).

in some Pyrenean massifs have been dated, yielding late Neoproterozoic–Early Cambrian ages (Rb–Sr method in the Agly paragneisses, see Table 1). According to Autran and Guitard (1996), these ages represent a Cadomian homogeneization of the Rb–Sr system superposed on older Precambrian protoliths (Sm–Nd model age of 1.6 Ga, Othman et al., 1984).

For the upper part of the sequence, a Mid–Late Cambrian age (Abad, 1987; Laumonier, 1988) or Late Cambrian/Early Ordovician (Guitard et al., 1998) has been proposed. Early Cambrian fossils have been found in an isolated outcrop located in the Eastern Pyrenees and bounded by Alpine faults (Abad, 1988; Perejón et al., 1994). However, the lack of continuity of this outcrop with the neighbouring massifs precludes any correlation with the pre-Upper Ordovician successions of the Pyrenees. Recent radiometric dating of an interlayered metatuff has yielded a Neoproterozoic age (581 Ma) for the middle part of the succession (U–Pb SHRIMP in zircon, Cocherie et al., 2005; see Table 1). This age measurement has rekindled the controversy over the existence of a Cadomian basement and had raised other interesting questions such as the position of the Neoproterozoic–Cambrian boundary, the age of the upper part of the succession, and the extent and the significance of the Upper Ordovician unconformity (Casas and Fernández, 2007).

Cocherie et al. (2005) also present some SHRIMP results obtained from inherited zircon in the igneous rocks, which have a variety of Pan-African (600–800 Ma), Mesoproterozoic (~1.0 Ga), Paleoproterozoic (~2.0 Ga) and Archean ages (2.5, 2.8 and 3.5 Ga).

4. SHRIMP U–Pb geochronology

4.1. Analytical techniques

U–Th–Pb analyses of zircon were conducted on the Sensitive High Resolution Ion Microprobe-Reverse Geometry (SHRIMP-RG) operated by the SUMAC facility (USGS-Stanford University) during one analytical session in February 2006.

Mineral separation was performed at the Universidad Complutense (Madrid) and the U.S. Geological Survey (Denver). The samples were crushed using a jaw crusher and pulverized with a disc mill. The zircons were separated using heavy fraction enrichment on a Wilfley table, magnetic separation with a Frantz isodynamic separator and density separation with methylene iodide. The zircons were handpicked under a binocular microscope and representative grains were chosen in accordance with size, length-to-breadth ratio, roundness, colour, and other salient morphological features. They were then mounted on a double-sided adhesive on glass slides in 1×6 mm parallel rows together with some chips of zircon standard R33 (Black et al., 2004). After being set in epoxy resin, the zircons were ground down to expose their central portions. Internal structure, inclusions, fractures and physical defects were identified with transmitted and reflected light on a petrographic microscope, and with cathodoluminescence on a JEOL 5800LV electron microscope (housed at USGS-Denver).

The mounted grains were washed with 1 N HCl and distilled water, dried in a vacuum oven, and coated with Au. Mounts typically sit in a loading chamber at high pressure (10^{-7} Torr) for several hours before being moved into the source chamber of the SHRIMP-RG.

Secondary ions generated from the target spot with an O^{2-} primary ion beam varying from 4–6 nA. The primary ion beam produced a spot with a diameter of ~25 μm and a depth of 1–2 μm for an analysis time of 8–10 min. Twelve peaks were measured sequentially in a single collector: $^{90}Zr_2^{16}O$, ^{204}Pb, background (0.050 mass units above ^{204}Pb), ^{206}Pb, ^{207}Pb, ^{208}Pb, ^{238}U, $^{248}Th^{16}O$, $^{254}U^{16}O$, $^{166}Er^{16}O$, $^{172}Yb^{16}O$, $^{180}Hf^{16}O$. Five scans were collected, and the counting time for ^{206}Pb was increased according to the Paleozoic age of the samples to improve counting statistics and precision of the $^{206}Pb/^{238}U$ age. Measurements were made at mass resolutions of 6000–8000 (10% peak height) which eliminates all interfering atomic species. The SHRIMP-RG employs magnetic analysis of the secondary beam before electrostatic analysis to provide higher mass resolution than the forward geometry of the SHRIMP I and II (Clement and Compston, 1994). The reverse geometry of the USGS-Stanford SHRIMP provides very clean backgrounds. This geometry combined with the high mass resolution and the acid washing of the mount ensures that surface contamination is removed and that counts found at mass ^{204}Pb are in fact Pb from the zircon. Moreover, before collecting the data the primary beam was rastered for 90–120 s over the area to be analyzed. Concentration data for zircons are standardized against zircon standard CZ3 (550 ppm U, Pidgeon et al., 1995), and isotope ratios were calibrated against R33 ($^{206*}Pb/^{238}U = 0.06716$, equivalent to an age of 419 Ma, Black et al., 2004) which were analyzed repeatedly throughout the duration of the analytical session.

Data reduction follows the methods described by Williams (1998) and Ireland and Williams (2003), and SQUID (version 1.08) and ISOPLOT (version 3.00) software (Ludwig, 2001, 2003) were used. The Pb composition used for initial Pb corrections was $^{204}Pb/^{206}Pb = 0.0554$, $^{207}Pb/^{206}Pb = 0.864$ and $^{208}Pb/^{206}Pb = 2.097$, calculated by SQUID using the age of the standard R33 and Stacey and Kramers (1975) model.

4.2. Sample descriptions

The metatuff collected in the Canigó massif (NU-3) has a medium-grained schistose fabric defined by lepidoblastic biotite-rich layers and granoblastic quartz-feldspathic domains, enclosing porphyroclasts of plagioclase, quartz and K-feldspar. Other minerals of this metamorphic paragenesis include muscovite and opaque ore. Chlorite and sericite replace biotite and feldspar, respectively.

In this sample, zircon morphologies vary from rounded grains to idiomorphic prisms, suggesting multiple zircon sources, consistent with a volcano-sedimentary origin of the host rock. Under cathodoluminescence (CL), most zircons exhibit oscillatory zoning and

xenocrystic cores (Fig. 3), although other textures, such as soccer-ball (grain 19) and homogeneous (grain 22) zoning can also be found.

The metatuff collected in the Roc de Frausa massif (RF-3) consists of variably recrystallized plagioclase porphyroclasts in a lepidoblastic groundmass of biotite, defining a planar fabric. Quartz, muscovite and opaque ore can also be found. Retrograde chlorite and sericite replace biotite and plagioclase. Zircons from sample RF-3 are moderately rounded stubby prisms (aspect ratio 1:2) and elongated prisms (aspect ratio 1:4). Under CL, these zircons display a faint moderately luminiscent oscillatory zoning with scarce xenocrystic weakly luminescent cores (Fig. 4).

The Mas Blanc orthogneiss (RF-4) contains centimetre-scale K-feldspar porphyroclasts in a heterogranular matrix composed of quartz, K-feldspar, plagioclase, biotite and garnet. Quartz has undulose extinction and subgrains, evidencing dynamic recrystallization. Secondary chlorite, clinozoisite, epidote and sericite are found. The Roc de Frausa orthogneiss (RF-5) is characterized by the presence of K-feldspar in a groundmass composed of quartz, plagioclase, biotite and garnet.

Zircons from the Mas Blanc and Roc de Frausa orthogneisses (RF-4 and RF-5, respectively) are similar: moderately rounded prisms with variable aspect ratios (1:2 to 1:4). CL images of both samples reveal an oscillatory zoning with some inherited xenocrystic cores (Fig. 4).

The Cap de Creus metatuff (CC-2) was sampled from a metre-scale lense of strongly foliated rocks with K-feldspar and albite porphyroclasts enclosed in a fine-grained matrix formed by abundant quartz, plagioclase, biotite and opaque minerals. Clinozoisite, sericite and chlorite replace the metamorphic mineral assemblage.

Zircons from this sample are stubby grains (aspect ratio lower than 1:2) with scarce inclusions and moderately rounded tips. Under CL a variety of textures become evident (Fig. 5), which is consistent with a volcano-sedimentary origin of this rock. These textures include oscillatory, sector (grain 15) and soccer-ball zoning (grain 17). Some grain cores are surrounded by a moderately luminiscent homogeneous rim (grain 9).

The Port orthogneiss (CC-7) is a highly homogeneous, massive and rather leucocratic sill. It displays a recognizable relict porphyritic texture with sporadic K-feldspar phenocrysts. The rock has a blasto-porphyritic texture, with tectonically induced foliation. The orthogneiss is composed of perthitic microcline, quartz, plagioclase and biotite. Accessory minerals are zircon, apatite, allanite and abundant titanite. Porphyroclasts composed of microcline containing amphibole, chlorite and albite inclusions and others consisting of polycrystalline albite are frequent.

In the Port gneiss, zircon grains are usually idiomorphic prisms (aspect ratios between 1:2 and 1:3) with small inclusions, although rounded grains and broken prisms can also be found. Under transmitted light microscopy, core-rim features are evident in some grains. Cathodoluminescence images reveal that most of the grains exhibit complex textures, commonly rounded xenocrystic cores with variable CL response, from low to high luminescence, and weakly luminescent overgrowths (Fig. 5). Other grains show oscillatory zoning with a varied luminescence response from core (moderate) to rim (weak).

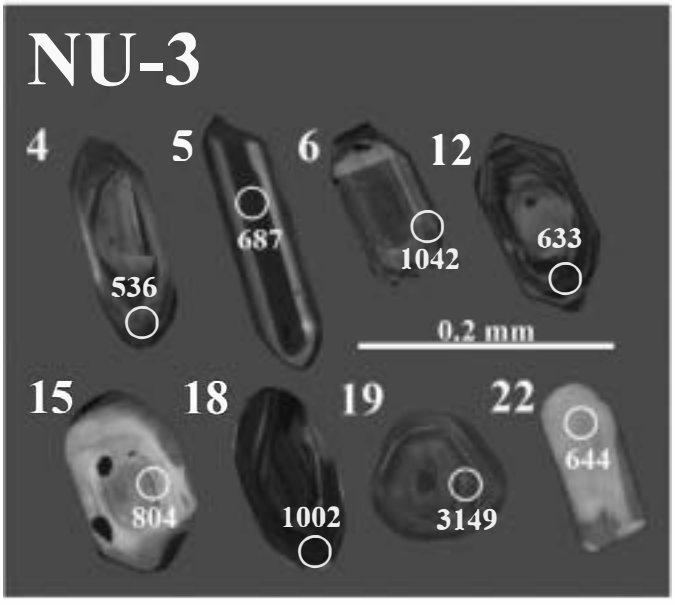

Fig. 3. Cathodoluminescence images of selected analyzed zircons from Núria (sample NU-3) with the location of the SHRIMP spots.

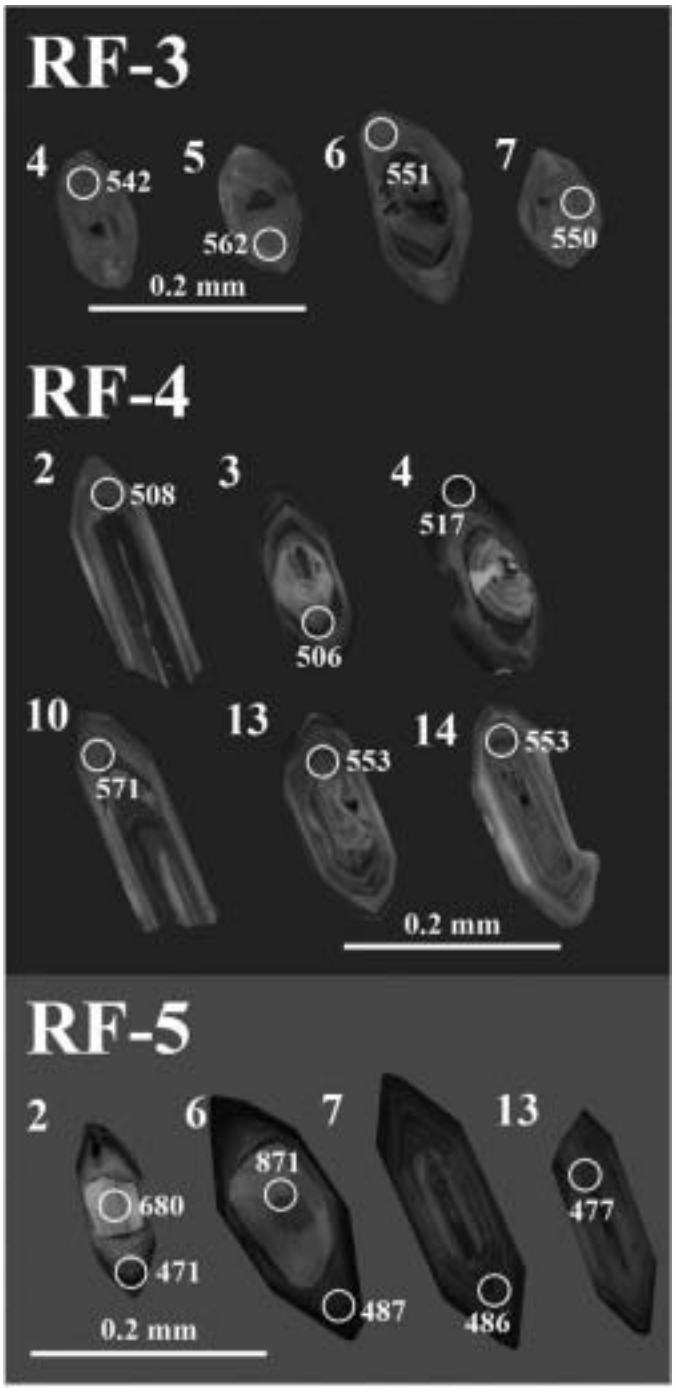

Fig. 4. Cathodoluminescence images of selected analyzed zircons from Roc de Frausa (samples RF-3 to RF-5) with the location of the SHRIMP spots.

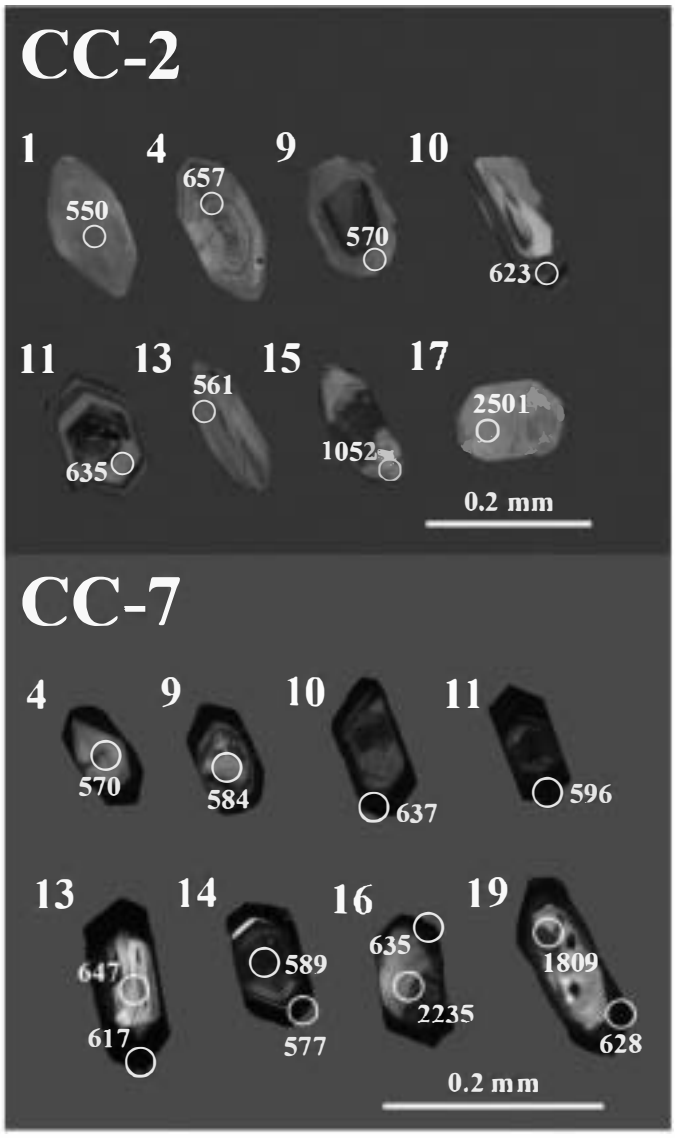

Fig. 5. Cathodoluminescence images of selected analyzed zircons from Cap de Creus (samples CC-2 and CC-7) with the location of the SHRIMP spots.

4.3. U–Pb results

One hundred and nine analyses were performed on 101 zircon grains. The whole set of analytical data is provided as supplementary material. Uncorrected radiogenic compositions are plotted in Tera–Wasserburg concordia diagrams (Figs. 6, 7 and 8). In order to visualize their complexity, results from some samples are also plotted in probability density diagrams (Fig. 9). Ages younger than 1000 Ma are reported as ^{207}Pb-corrected ^{206}Pb/^{238}U. Otherwise, the reported age is ^{204}Pb-corrected ^{207}Pb/^{206}Pb. The correction method is described in Ludwig (2001).

In the metatuff from the Canigó massif (NU-3), the variety of zircon textures results in an assortment of ages (Fig. 6) that can be clearly visualized in a probability density diagram (Fig. 9), where data with less than 10% of discordance were plotted. In this plot, the age profile presents significant peaks at ~640, ~680, ~800 and ~970 Ma. In addition, some older ages can also be found, with peaks at ~1.0, ~2.3 (with a discordance greater than 10%, and therefore not included in Fig. 9) and 3.1 Ga.

Because of its volcanoclastic nature, it is not possible to obtain an exact age for this sample. Instead, a maximum age could be inferred for its formation, considering the youngest concordant age obtained from a magmatic zircon. However, the youngest age in this sample corresponds to a single analysis (~540 Ma, Fig. 3, grain 4), which makes it unsuitable for inferring the maximum deposition age of sample NU-3 owing the possibility of lead loss. The next youngest age group clusters around an age of 640 Ma, which is too old to be considered close to the deposition age given earlier geochronological work (see above).

In the Roc de Frausa massif, the results in the metatuff (sample RF-3) and the Mas Blanc orthogneiss (sample RF-4) are dominated by Neoproterozoic to Early Cambrian ages, whereas, data from the Roc de Frausa orthogneiss (sample RF-5) yield an Early Ordovician age and a string of Neoproterozoic inheritances (Figs. 7, 9). In sample RF-3, only weakly luminescent areas with oscillatory zoning were analyzed to obtain the protolith crystallization age. The analyzed areas have low U contents (90–140 ppm) and a tight range of Th/U ratios (0.3–0.4). Even though their measured isotopic compositions are concordant within analytical uncertainty (Fig. 7a) the best age is obtained from a set of seven analyses, yielding a concordia age of 548.4±8.4 Ma (95% confidence). The outlier analyses are omitted owing to their high U content (points 9.1 and 11.1), the low Th/U ratio (point 10.1) and the possibility of lead loss (point 1.1).

In the Mas Blanc orthogneiss (RF-4), the analyzed spots correspond to weakly luminescent magmatic oscillatory zones with moderate U content (150–800 ppm) and Th/U ratios (0.09–0.35). The measured radiogenic compositions are equally distributed between two populations, ~510 and ~560 Ma. There are two possible explanations for this arrangement: 1) the younger age could represent the crystallization age with the result that the older one would be interpreted as inheritance; 2) the older age could be regarded as the crystallization age and the younger age would reflect lead loss. There appears to be no relation between age difference and CL features (Fig. 4), common lead, uranium, thorium contents or Th/U ratio, which is to be expected in zircons grown at different times (see Supplementary material). Thus, we prefer the latter interpretation and consider that ~560 Ma represents the crystallization age of the igneous protolith. By pooling the oldest ages, we obtain a concordia age of 560.1±7.2 Ma (95% confidence) for the crystallization of this rock.

In the Roc de Frausa orthogneiss (RF-5), twelve analyses were made in moderately luminescent areas with oscillatory zoning to obtain the crystallization age of the protolith. The U content and the Th/U ratio vary widely in range (100–1200 ppm and 0.07–2.30, respectively). After rejecting analyses 5.1, 10.1, 12.1 (probable

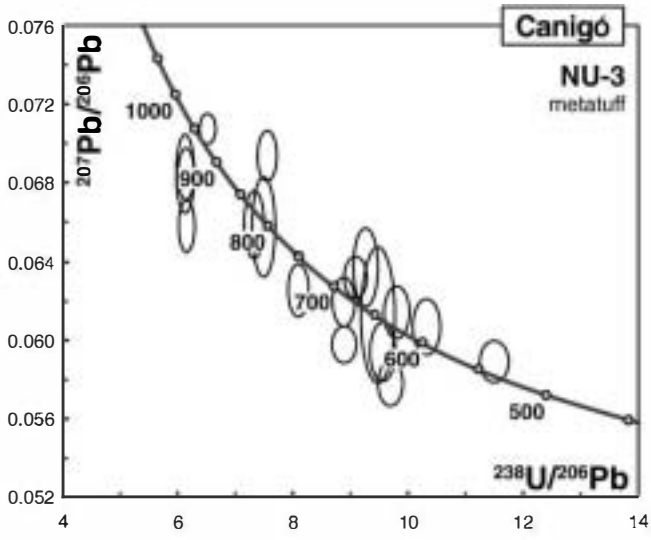

Fig. 6. Tera–Wasserburg plot showing distribution of SHRIMP zircon analyses from sample NU-3 from Núria. Five older inheritance ages are not shown for clarity. Error ellipses are ±1σ.

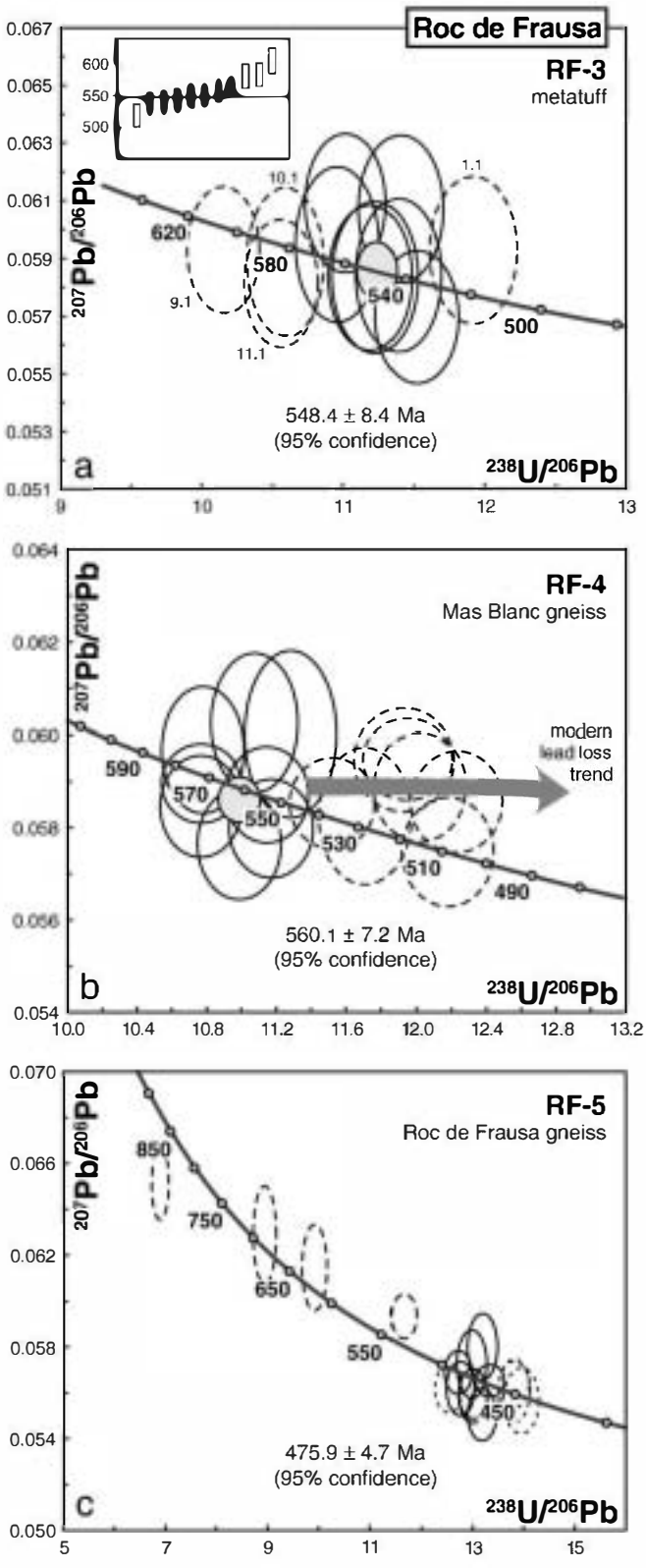

Fig. 7. Tera–Wasserburg plots showing distribution of SHRIMP zircon analyses from samples from Roc de Frausa, a RF-3, dashed ellipses represent discarded analyses to obtain the concordia age (inset), b RF-4, dashed ellipses represent lead loss affected analyses, c RF-5, dashed ellipses are inheritance and discarded analyses to obtain the mean age. The grey solid ellipses represent the concordia age (sensu Ludwig, 1998). Error ellipses and bars are ±1σ.

lead loss) and 1.2 (probable hit in a core), a mean age of 475.9 ± 4.7 Ma (95% confidence) was obtained from eight analyses (Fig. 7c). Additionally, four xenocrystic cores were analyzed to trace the inheritance component, yielding single ages in the interval from ~530 to ~870 Ma (Fig. 9).

In the Cap de Creus metatuff (CC-2), the range of ages obtained is attributed to the diverse CL textures found in zircon grains. The spots were aimed to magmatic areas with oscillatory or homogeneous zoning, avoiding weakly luminescent rims. The U and Th contents of the analyzed grains are low to moderate, with Th/U ratios typical of melt-precipitated zircon. The youngest set of analyses yields a concordia age (sensu Ludwig, 1998) of 560.1 ± 10.7 Ma (Fig. 8a). The remaining results are inherited ages in the 600–900 Ma and 2.5 Ga ranges (Fig. 9). In the Port orthogneiss (CC-7), 21 grains were analyzed in the central and rim areas with oscillatory zones, hitting some xenocrystic cores to trace inheritance. The U and Th contents of the analyzed spots are variable, ranging 100–7000 ppm and 50–1900 ppm, respectively (see Supplementary material). The measured radiogenic $^{206}Pb/^{238}U$ values are equivalent to ages from 540 to 2500 Ma. Bearing these parameters in mind, three groups can be differentiated (Fig. 10). The first group is composed of analyses with the lowest $^{206}Pb/^{238}U$ values and moderate U and Th contents obtained from spots in the

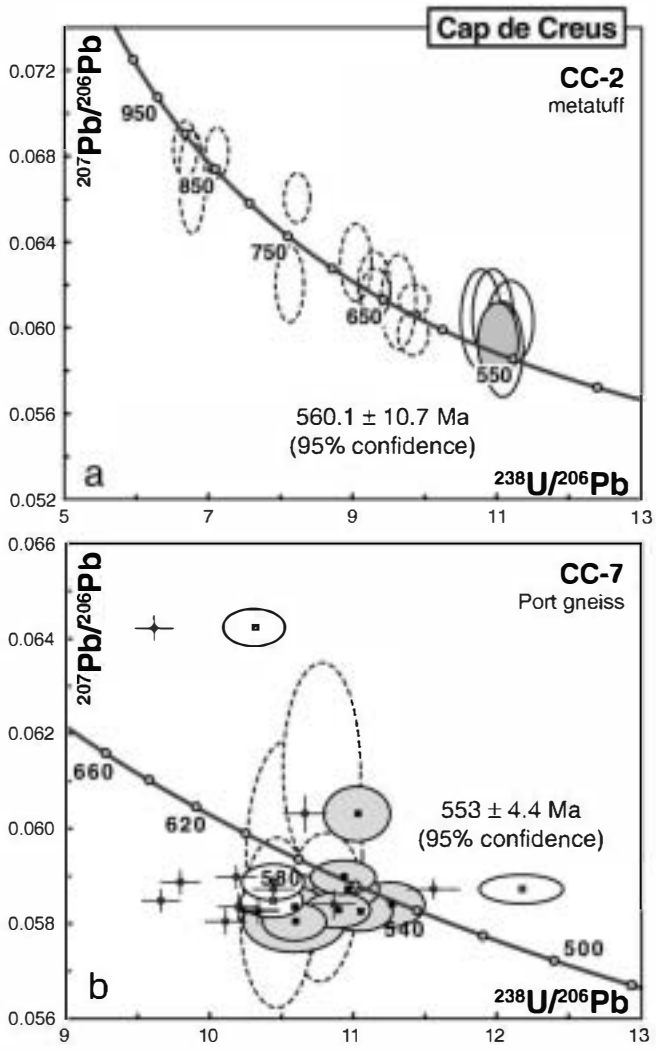

Fig. 8. Tera–Wasserburg plots showing distribution of SHRIMP U–Pb zircon ages from samples from Cap de Creus, a) sample CC-2, the grey solid ellipse represents the concordia age (sensu Ludwig, 1998), calculated using the solid ellipse analyses; dashed ellipses represent inheritance; b) sample CC-7; dashed ellipses, group I analyses; circles with error bars represent group III uncorrected analyses; grey ellipses, group III corrected analyses used to calculate the mean age; white ellipses, group III corrected analyses discarded for the mean age calculation. Seven older inherited ages (group II) are not shown for clarity. Error ellipses are ±1σ.

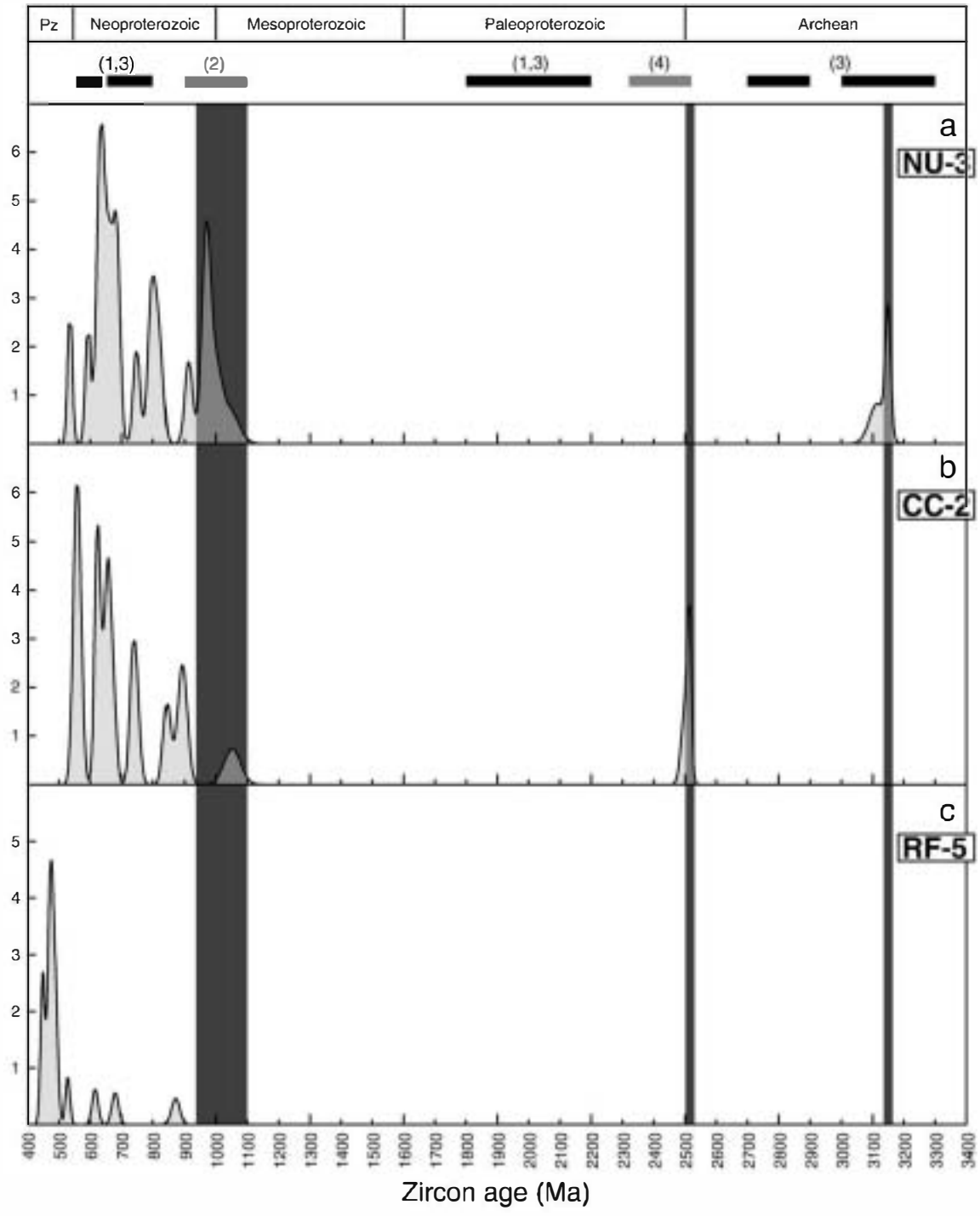

Fig. 9. Relative probability plots of U–Pb ages for detrital and inherited zircons from two metatuffs (a, CC-2; b, NU-3) and a granitic orthogneiss (c, RF-5).For comparison, the age distributions of Northern (in grey) and Western Africa (in black) are shown. Data sources: 1, Fernández-Suárez et al. (2000); 2, Avigad et al. (2003); 3, Linnemann et al. (2004); 4, Abdesalam et al. (2002).

central areas of magmatic zircons (points 4.1, 8.1, 9.1, 14.2 and 20.1). Isotopic ratios form a cluster giving a mean age of 576±8 Ma (95% confidence). The second group has also moderate U and Th contents, and ages range from 620 to 2500 Ma (interpreted as inheritance). The analyses were made in xenocrystic cores (points 13.2,16.2, 19.2 and 21.2) and zircon magmatic grains without weakly luminescent (metamorphic) rims (points 2.1, 3.1 and 12.1). The third group has high U contents (over 4000 ppm) obtained from spots in weakly luminescent magmatic rims. The reverse discordance of these analyses (Fig. 8) and the strong correlation between U and radiogenic $^{206}Pb/^{238}U$ (Fig. 10), suggest that these are more probably due to U-dependent changes in sputtering and secondary ionization efficiency than to accumulated radiation damage (Butera et al., 2001). This situation resembles that described in McLaren et al. (1994) and Williams and Hergt (2000). This analytical bias can be compensated, applying a correction of 2% per 1000 ppm of U over 2500 ppm (see Supplementary material), which reduces the dispersion in radiogenic $^{206}Pb/^{238}U$ (Fig. 8). However, to obtain a weighted mean $^{206}Pb/^{238}U$ age we must reject some of the analyses with the highest U and Th (points 10.1, 15.1, 16.1, 18.1 and 19.1). The youngest age was ruled out (point 1.1) because it deviated from the

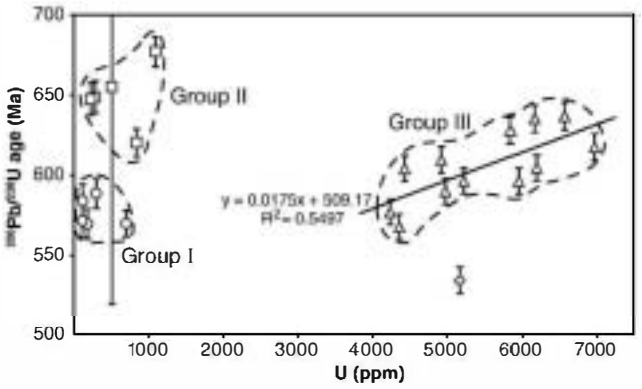

Fig. 10. $^{206}Pb/^{238}U$ age versus U content for the Port gneiss sample (CC-7), where three groups can be visualized.

correlation trend (Fig. 10). The remaining six analyses had a weighted mean age of 558.4±6.3 Ma (95% confidence).

Given that $^{207}Pb/^{206}Pb$ ratios are not affected by the U content, as noted by McLaren et al. (1994), a weighted mean can be calculated for all the high U analyses (except 16.1), yielding an age of 546±7.3 Ma (95% confidence), equivalent within error to the $^{206}Pb/^{238}U$ age. By pooling both ages, we can obtain a best estimate of 553±4.4 Ma (95% confidence) for the protolith age of the Port orthogneiss. Finally, older ages ranging from 1.8 to 2.5 Ga are regarded as inheritance.

5. Interpretation and discussion

5.1. Zircon inheritance

Despite of the scarcity of inherited ages obtained in the Canigó and Cap de Creus metatuffs (samples NU-3, and CC-2) and the Roc de Frausa orthogneiss (sample RF-5), some conclusions on the characterization of the sedimentary sources can be drawn. The presence of Pan-African (600–800 Ma) and Mesoarchean (~3.1 Ga) detrital zircon ages point to a West African craton provenance, which is similar to other peri-Gondwanan areas (e.g., Fernández-Suárez et al., 2002b; Linnemann et al., 2004). However, the Grenvillian (0.9–1.1 Ga) signature in the detrital zircon age patterns in the Neoproterozoic and Paleozoic sediments of the Variscan belt has been used to lend support to the existence of South American derived crust in Central Europe (Friedl et al., 2000). Fernández-Suárez et al. (2002b) and Gutiérrez-Alonso et al. (2003) have proposed two contrasting source areas during the Neoproterozoic in the pre-Variscan exposures of the Iberian massif: the West African craton for the Ossa–Morena zone and the South American craton for the Cantabrian, West Asturian Leonese and Central Iberian zones. This paleogeographic model is supported by the presence of Grenvillian ages in detrital zircons and by the higher ε_{Nd} values in the South American derived zones. This is not consistent with the absence of Grenvillian ages and the lower ε_{Nd} values in the West African derived zone.

However, this is not the only explanation to account for a Grenvillian signature in the detrital zircon spectra of samples from the Peri-Gondwana realm. Recently, some authors have documented Grenville zircon ages in sediments from northern Gondwana, at a considerable distance from Amazonian sources, favouring a North African source (Keay and Lister, 2002; Avigad et al., 2003; Drost et al., 2007).

Finally, Neoarchean ages (~2.5 Ga) can be found in both Amazonian and North African sources (Abdesalam et al., 2002; Fernández-Suárez et al., 2002a).

5.2. Age of the pre-Upper Ordovician sequences and magmatism in the Pyrenees

Based on our geochronological data, we recognize two pre-Variscan magmatic episodes related to the pre-Upper Ordovician sequence. The oldest magmatic episode is represented by intrusive and extrusive rocks. The results from the extrusive rocks yield information on the age of the sequences. Thus, from the Cap de Creus metatuff (CC-2) we estimate the age of the top of the Lower Series to be at least 560 Ma.

In the Upper Series of the Roc de Frausa massif, the results from an interbedded metatuff (sample RF-3) indicate that it was deposited approximately at ~548 Ma, close to the Ediacaran–Cambrian boundary. To the SW of the Canigó massif, the analyzed metatuff (NU-3) occupies an equivalent stratigraphic position of sample RF-3. However, owing to the abundance of inherited zircon grains, only one analysis yielded an age close to ~540 Ma, making it difficult for us to obtain a maximum deposition age. Cocherie et al. (2005) analyzed zircons that also provided ~545 Ma in an equivalent sample from the southern slope of the Canigó massif (GRA-1). These authors discarded this result in favour of an older age of 580 Ma, arguing that it was difficult to regard all the zircons dated between 570 and 600 Ma as inherited zircons. This is a surprising statement given the continued Cadomian igneous activity from 600 to 550 Ma along the northern Gondwana margin.

In the light of these findings, it is reasonable to assume that the Neoproterozoic–Cambrian boundary is situated fairly close to the studied samples in the three massifs. In the Canigó massif it would be located inside the Canavelles Series, probably in the lithologically varied group (black shales, carbonates and metavolcanic rocks) located in the lower part of the Canavelles Series, where sample NU-3 was collected (Fig. 2). In the Roc de Frausa, the presence of a syn-orogenic Variscan granitoid masks the upper part of the metasedimentary series. However, this boundary would be situated in the Upper series close to sample RF-3 (Fig. 2). In Cap de Creus, the presence of the Roses and Rodes granodiorites and the reduced thickness of the series make it more difficult to place the boundary. However, it could be located in the conglomerates and carbonates of the Upper series (Fig. 2). Should this interpretation be correct, the Jujols Series of Cavet (1957), or Jujols Group of Laumonier et al. (2004) could represent a sequence deposited in a quiet environment, probably ranging in age from Mid Cambrian to Early Ordovician (Fig. 2). Nevertheless, further research and geochronological work is needed to assess the age of the intermediate levels of the Canavelles and Jujols Series and the magnitude of the Upper Ordovician unconformity.

Moreover, the metaplutonic rocks located in the lower part of the series in the Cap de Creus and Roc de Frausa massifs (Port and Mas Blanc orthogneisses, respectively) yield Late Neoproterozoic ages for their intrusion (553 and 560 Ma, respectively). These ages correspond to the emplacement of the plutonic rocks, and are roughly equivalent to the age of the metatuffs interbedded in the upper part of the metasedimentary sequence. However, the age of the lowermost series in the three massifs remains unresolved, even though an age slightly older than the plutonic rocks could be proposed (older than 600 Ma?). Further geochronological studies are warranted to gain further insight into the age of these series that represent the deepest rocks cropping out in the Eastern Pyrenees.

Field relationships and geochemistry of metatuffs, metabasites and metaplutonic rocks suggest that this syn-sedimentary Late Neoproterozoic (Ediacaran)–Early Cambrian magmatism is bimodal. No tectonic or metamorphic Late Neoproterozoic–Early Cambrian activity related to this igneous event has been described in the study area, to date.

The second magmatic episode is represented by sample RF-5 (Roc de Frausa gneiss) which yields 476 Ma, confirming the presence of an important Early Ordovician magmatic event. This event is recognized in the Pyrenees (Delaperrière and Respaut, 1995; Deloule et al., 2002; Cocherie et al., 2005) and in other sectors of the European Variscides, where the intrusion of Early Ordovician granites is widely documented (Delaperrière and Lancelot, 1989; Pin and Marini, 1993; Valverde-Vaquero and Dunning, 2000; Roger et al., 2004; Helbing and Tiepolo,

2005; Castiñeiras et al., 2008). The intrusion of Early Ordovician granites is apparently unrelated to any deformational or metamorphic episode and predates the Upper Ordovician unconformity.

These ages are in agreement with the models proposed for the pre-Variscan evolution in the Central and Southeastern European Alpine mountain belts. In these models, an Andean-type continental margin triggered by the southward subduction of the Iapetus or Proto-Thethys Ocean (570–520 Ma) is followed by a back-arc rifting episode (520–500 Ma) prior to the separation of a terrane from northern Gondwana (490–485 Ma) (Neubauer, 2002; Stampfli et al., 2002; von Raumer et al., 2002). Cambrian igneous activity related to a rifting episode is widespread in the Iberian massif (Simancas et al., 2004), but it has not been recognized in the Pyrenees to date.

In addition, the subsidence pattern from Lower Ordovician to Carboniferous calculated by von Raumer and Stampfli (2008-this issue) for the Pyrenees documents the continuation of the extensional episode and the opening of the Paleotethys.

6. Concluding remarks

U–Pb SHRIMP dating of metaigneous rocks from the pre-Variscan basement enabled us to differentiate two magmatic episodes. The older episode is constituted by Late Cadomian intrusive and extrusive rocks (560–580 Ma), whereas the younger episode corresponds to Early Ordovician magmatism (476 Ma).

The ages obtained in extrusive rocks from the pre-Upper Ordovician metasedimentary sequence for the series of the Roc de Frausa and Cap de Creus massifs allow us to estimate the deposition age as Ediacaran–Early Cambrian (>540 Ma). In the Canigó massif, this age would correspond to the lower part of the Canavelles series. We suggest that the lowermost series of the three massifs (Balaig series, in the Canigó and the Lower and Intermediate series in the Roc de Frausa and Cap de Creus massifs) are Neoproterozoic. It should be noted that neither of the two magmatic episodes described can be related to deformational structures. All this confirms the absence of a Cadomian basement in the Pyrenees.

Moreover, despite the scarcity of inherited zircon ages; these ages are sufficiently distinctive to identify a source for the metavolcano-sedimentary rocks from the Eastern Pyrenean massifs. This source may be comparable with the Cantabrian, West Asturian Leonese and Central Iberian zones in the Iberian Massif, and would probably be located in North Africa.

Acknowledgements

The authors are grateful to all the staff at the SUMAC facility for their assistance during the SHRIMP-RG analytical sessions, especially J. Wooden and F. Mazdab. This work has been supported by the Spanish Commission for Science and Technology, project BTE2003-08653-CO2, CGL-2007-66857CO2-02 and the Consolider-Ingenio 2010 programme, under CSD2006-00041 "Topoiberia". The study was undertaken while P. Castiñeiras was holding a Fulbright postdoctoral fellowship at the University of Colorado, funded by the Spanish Ministerio de Educación y Ciencia. P. Castiñeiras is indebted to I. Brownfield, at the USGS-Denver Microbeam Laboratory, for her help during the CL imaging of the zircons. J. Aleinikoff and W. Premo provided the necessary equipment to prepare and image the SHRIMP mounts, helped with the presentation and interpretation of isotopic data, and with the English version. An earlier version of this manuscript was improved thanks to the exhaustive revision of Jürgen von Raumer and an anonymous referee.

Appendix A. Supplementary data

Supplementary data associated with this article can be found, in the online version, at doi:10.1016/j.tecto.2008.04.005.

References

Abad, A., 1987. Primera cita de arqueociátidos en Cataluña. Trab. Mus. Geol. Semin. Barc. 222, 10.
Abad, A., 1988. El Cámbrico inferior de Terrades (Gerona). Estratigrafía, facies y paleontología. Batallería 2, 47–56.
Abdesalam, M.G., Liégeois, J.P., Stern, R.J., 2002. The Saharan metacraton. J. Afr. Earth Sci. 34, 119–136.
Autran, A., Guitard, G., 1969. Mise en évidence de nappes hercyniennes de style penninique dans la série métamorphique du massif du Roc de France (Pyrénées orientales): liaison avec la nappe du Canigou. C. R. Acad. Sci. Paris 269, 2479–2499.
Autran, A., Guitard, G., 1986. Les données géochronologiques isotopiques. In: Barnolas, A., Chiron, J.C. (Eds.), Synthèse géologique et géophysique des Pyrénées, vol. 1. BRGM-ITGE, Orléans, pp. 147–154.
Autran, A., Fonteilles, M., Guitard, G., 1970. Relations entre les intrusions de granitoides, l'anatexie, et le métamorphisme régional considerées principalment du point de vue de l'eau: cas de la Chaine hercynienne des Pyrénées Orientales. Bull. Soc. Géol. Fr. 7, 673–731.
Avigad, D., Kolodner, K., McWilliams, M., Persing, H., Weissbrod, T., 2003. Origin of northern Gondwana Cambrian sandstone revealed by detrital zircon SHRIMP dating. Geology 31, 227–230.
Ayora, C., Casas, J.M., 1986. Strabound As–Au mineralization in pre-Caradocian rocks form the Vall de Ribes, Eastern Pyrenees, Spain. Miner. Depos. 21, 278–287.
Bandrés, A., Eguíluz, L., Pin, C., Paquette, J.L., Ordóñez, B., Le Fèvre, B., Ortega, L.A., Gil Ibarguchi, J.I., 2004. The northern Ossa–Morena Cadomian batholith (Iberian Massif): magmatic arc origin and early evolution. Int. J. Earth Sci. 93, 860–885.
Barbey, P., Cheilletz, A., Laumonier, B., 2001. The Canigou orthogneisses (Eastern Pyrenees, France, Spain): an Early Ordovician rapakivi laccolith and its contact aureole. C. R. Acad. Sci. Paris 332, 129–136.
Black, L.P., Kamo, S.L., Allen, C.M., Davis, D.W., Aleinikoff, J.N., Valley, J.W., Mundil, R., Campbell, I.H., Korsch, R.J., Williams, I.S., Foudoulis, C., 2004. Improved $^{206}Pb/^{238}U$ microprobe geochronology by the monitoring of a trace-element-related matrix effect, SHRIMP, ID-TIMS, ELA-ICP-MS and oxygen isotope documentation for a series of zircon standards. Chem. Geol. 205, 115–140.
Butera, K.M., Williams, I.S., Blevin, P.L., Simpson, C.J., 2001. Zircon U–Pb dating of Early Paleozoic monzonitic intrusives from the Goonumbla area, New South Gales. Aust. J. Earth Sci. 48, 457–464.
Carreras, J., Ramírez, J., 1984. The geological significance of the Port de la Selva gneisses (Eastern Pyrenees, Spain). Newsletter - IGCP Project 5 6, 27–31.
Carreras, J., Losantos, M., Palau, J., Escuer, J., 1994. Memoria del Mapa geológico de España 1/50.000 (259 Roses). IGME, Madrid. 37 pp.
Casas, J.M., Fernández, O., 2007. On the Upper Ordovician unconformity in the Pyrenees: New evidence from the La Cerdanya area. Geol. Acta 5, 193–198.
Casas, J.M., Martí, J., Ayora, C., 1986. Importance du volcanisme dans la composition lithostratigraphique du Paléozoïque inférieur des Pyrénées catalanes. C. R. Acad. Sci. Paris 302, 1193–1198.
Castiñeiras, P., Villaseca, C., Barbero, L., Martín Romera, C., 2008. SHRIMP U–Pb zircon dating of anatexis in high-grade migmatite complexes of Central Spain: implications in the Hercynian evolution of Central Iberia. Int. J. Earth Sci. 97, 35–50.
Cavet, P., 1957. Le Paléozoïque de la zone axiale des Pyrénées orientales françaises entre le Roussillon et l'Andorre. Bull. Serv. Carte Geol. Fr. 254, 303–518.
Clement, S.W.J., Compston, W., 1994. Ion probe parameters for very high resolution without loss of sensitivity. U.S. Geol. Surv. Circ. 1107, 62.
Cocherie, A., Baudin, Th., Autran, A., Guerrot, C., Fanning, C.M., Laumonier, B., 2005. U–Pb zircon (ID-TIMS and SHRIMP) evidence for the early Ordovician intrusion of metagranites in the late Proterozoic Canaveilles Group of the Pyrenees and the Montagne Noire (France). Bull. Soc. Géol. Fr. 176, 269–282.
Delaperrière, E., Lancelot, J., 1989. Datation U–Pb sur zircons de l'orthogneiss du Capo Spartivento (Sardaigne, Italie), nouveau témoin d'un magamatisme alcalin ordovicien dans le sud de l'Europe. C. R. Acad. Sci. Paris 309, 835–842.
Delaperrière, E., Soliva, J., 1992. Détermination d'un âge Ordovicien supérieur-Silurien des gneiss de Casemi (Massif du Caigou, Pyrénées Orientales) par la méthode d'évaporation du plomb sur monozircon. C. R. Acad. Sci. Paris 314, 345–350.
Delaperrière, E., Respaut, J.P., 1995. Un âge ordovicien de l'orthogneis de La Preste par le méthode d'évaporation directed du plomb sur monozircon remet en question l'existence d'un socle précambrien dans le Massif du Canigou (Pyrénées Orientales, France). C. R. Acad. Sci. Paris 320, 1179–1185.
Delaperrière, E., Saint-Blanquat, M. (de), Brunel, M., Lancelot, J., 1994. Géochronologie U–Pb sur zircons et monazites dans le massif du Saint-Barthélémy (Pyrénées, France): discussion des âges des événements varisques et prévarisques. Bull. Soc. Géol. Fr. 165, 101–112.
Deloule, E., Alexandrov, P., Cheilletz, A., Laumonier, B., Barbey, P., 2002. In-situ U–Pb zircon ages for Early Ordovician magmatism in the eastern Pyrenees, France: the Canigou orthogneisses. Int. J. Earth Sci. 91, 398:405.
Díaz García, F., 2006. Geometry and regional significance of Neoproterozoic (Cadomian) structures of the Narcea antiform, NW Spain. J. Geol. Soc. Lond. 163, 499–508.
Drost, K., Gerdes, A., Jeffries, T., Linnemann, U., Romer, R., 2007. The Teplá–Barrandian unit (Bohemian Massif, central Europe): Part of the NW-African continental margin during the Neoproterozoic and Paleozoic? IGCP 485 and IGCP 497 Joint Conference, El Jadida (Morocco), pp. 29–30. Abstracts volumen.
Fernández-Suárez, J., Gutiérrez Alonso, G., Jenner, G., Simon, E.J., 1998. Geochronology and geochemistry of the Pola de Allende granitoids (northern Spain): their bearing on the Cadomian–Avalonian evolution of northwest Iberia. Can. J. Earth Sci. 35, 1439–1453.
Fernández-Suárez, J., Gutiérrez-Alonso, G., Jenner, G.A., Tubrett, M.N., 2000. New ideas on the Proterozoic–Early Palaeozoic evolution of NW Iberia: insights from U–Pb detrital zircon ages. Precambrian Res. 102, 185–206.

Fernández-Suárez, J., Gutiérrez-Alonso, G., Cox, R., Jenner, G.A., 2002a. Assembly of the Armorica microplate: a strike slip terrane delivery? Evidence from U–Pb ages of detrital zircons. J. Geol. 110, 619–626.

Fernández-Suárez, J., Gutiérrez-Alonso, G., Jeffries, T.E., 2002b. The importance of along-margin terrane transport in northern Gondwana: insights from detrital zircon parentage in Neoproterozic rocks from Iberia and Brittany. Earth Planet. Sci. Lett. 204, 75–88.

Fontboté, J.M., 1949. Nuevos datos geológicos sobre la cuenca alta del Ter. An. Inst. Est. Gerund. IV, 1–57.

Friedl, G., Finger, F., McNaughton, N.J., Fletcher, I.R., 2000. Deducing the ancestry of terranes: SHRIMP evidence for South America-derived Gondwana fragments in central Europe. Geology 28, 1035–1038.

Gerdes, A., Zeh, A., 2006. Combined U–Pb and Hf isotope LA-(MC-)ICP-MS analyses of detrital zircons: Comparison with SHRIMP and new constraints for the provenance and age of an Armorican metasediment in Central Germany. Earth Planet. Sci. Lett. 249, 47–61.

Guitard, G., 1970. Le métamorphisme hercynien mésozonal et les gneiss oeillés du massif du Canigou (Pyrénées-Orientales). BRGM. Mém. 63,353 pp.

Guitard, G., Laffitte, F., 1956. Sur l'importance et la nature des manifestations volcaniques dans le Paléozoïque des Pyrénées Orientales. C. R. Acad. Sci. Paris 242, 2749–2752.

Guitard, G., Autran, A., Fonteilles, M., 1996. Le substratum précambrien du Paléozoïque. In: Barnolas, A., Chiron, J.C. (Eds.), Synthèse géologique etgèophisique des Pyrénées, vol. 1. BRGM-ITGE, Orléans, pp. 137–156.

Guitard, G., Laumonier, B., Autran, A., Bandet, Y., Berger, G.M., 1998. Notice explicative, Carte géologique France (1:50.000), feuille Prades (1095). BRGM. Orléans. 198 pp.

Gutiérrez-Alonso, G., Fernández-Suárez, J., Jeffries, T., Jenner, G.A., Tubrett, M.N., Cox, R., Jackson, S.E., 2003. Terrane accretion and dispersal in the northern Gondwana margin. An Early Paleozoic analogue of a long-lived active margin. Tectonophysics 365, 221–232.

Hartevelt, J.J.A., 1970. Geology of the Upper Segre and Valira valleys, Central Pyrenees, Andorra/Spain. Leidse Geol. Meded. 45, 167–236.

Helbing, H., Tiepolo, M., 2005. Age determination of Ordovician magmatism in NE Sardinia and its bearing on Variscan basement evolution. J. Geol. Soc. Lond. 162, 689–700.

Ireland, T.R., Williams, I.S., 2003. Considerations in zircon geochronology by SIMS. In: Hanchar, J.M., Hoskin, P.W.O. (Eds.), Zircon. Mineralogical Society of America, Washington. Rev. Mineral. Geochem., vol. 53, pp. 215–241.

Jäger, E., Zwart, H.J., 1968. Rb–Sr age determinations of some gneiss and granites of the Aston–Hospitalet massif (Pyrenees). Geol. Mijnb. 47, 349–357.

Keay, S., Lister, G., 2002. African provenance for the metasediments and metaigneous rocks of the Cyclades, Aegean Sea, Greece. Geology 30, 235–238.

Laumonier, B., 1988. Les groupes de Canaveilles et de Jujols («Paléozoïque inférieur ») des Pyrénées orientales. Arguments en faveur de l'âge essentiellement cambrien de ces séries. Hercynica 4, 25–38.

Laumonier, B., Autran, A., Barbey, P., Cheilletz, A., Baudin, Th., Cocherie, A., Guerrot, C., 2004. Conséquences de l'absence de socle cadomien sur l'âge et la signification des séries pré-varisques (anté-Ordovicien supérieur) du sud de la France (Pyrénées, Montagne Noire). Bull. Soc. Géol. Fr. 175, 643–655.

Liesa, M., Carreras, J., 1989. On the structure and metamorphism of the Roc de Frausa Massif (Eastern Pyrenees). Geodin. Acta 3, 149–161.

Linnemann, U., McNaughton, N.J., Romer, R.L., Gehmlich, M., Drost, K., Tonk, C., 2004. West African provenance for Saxo–Thuringia (Bohemian Massif): did Armorica ever leave pre-Pangean Gondwana? — U/Pb-SHRIMP zircon evidence and the Nd-isotopic record. Int. J. Earth Sci. 93, 683–705.

Losantos, M., Palau, J., Carreras, J., Druguet, E., Santanach, P., Cirés, J., 1997. Mapa Geològic de Catalunya 1:25000. Full259-2-1 (Cap de Creus). Institut Cartogràfic de Catalunya.

Ludwig, K.R., 1998. On the treatment of concordant uranium–lead ages. Geochim. Cosmochim. Acta 62, 665–676.

Ludwig, K.R., 2001. SQUID 1.02, a user's manual. Berkeley Geochronology Center. Special Publication 2, 17 pp.

Ludwig, K.R., 2003. ISOPLOT/Ex, version 3, A Geochronological Toolkit for Microsoft Excel. Berkeley Geochronology Center. Special Publication 4, 71 pp.

Majoor, F.J.M., 1988. On the age and origin of the Aston gneiss massif, Central Pyrenees. Hercynica 4, 57–61.

Marshall, R., 1987. The Hercynian of the Pyrenees, was it really extending? Terra Cogn. 7, 315.

McLaren, A.C., Fitz Gerald, J.D., Williams, I.S., 1994. The microstructure of zircon and its influence on the age determination from Pb/U isotopic ratios measured by ion microprobe. Geochim. Cosmochim. Acta 58, 993–1005.

Muñoz, J.A., Casas, J.M., 1996. Tectonique préhercynienne. In: Barnolas, A., Chiron, J.C. (Eds.), Synthèse géologique et géophysique des Pyrénées, vol. 1. BRGM-ITGE, Madrid, pp. 587–589.

Murphy, J.B., Pisarevsky, S.A., Nance, R.D., Keppie, J.D., 2004. Neoproterozoic–Early Paleozoic evolution of peri-Gondwanan terranes: implications for Laurentia–Gondwana connections. Int. J. Earth Sci. 93, 659–682.

Nägler, T.F., Shäfer, H.J., Gebauer, D., 1995. Evolution of the Western European continental crust: implications from Nd and Pb isotopes in Iberian sediments. Chem. Geol. 121, 345–347.

Navidad, M., Carreras, J., 1995. Pre-Hercynian magmatism in the eastern Pyrenees (Cap de Creus and Albera Massifs) and its geodynamical setting. Geol. Mijnb. 74, 65–77.

Navidad, M., Carreras, J., 2002. El volcanismo de la base del Paleozoico Inferior del Canigó (Pirineos Orientales). Evidencias geoquímicas de la apertura de una cuenca continental. Geogaceta 32, 91–94.

Navidad, M., Liesa, M., Carreras, J., 1996. Magmatismo Paleozoico en el Macizo del Roc de Frausa (Pirineos Orientales). Acta Geol. Hisp. 31, 1–15.

Neubauer, F., 2002. Evolution of late Neoproterozoic to early Paleozoic tectonic elements in Central and Southeast European Alpine mountain belts: review and synthesis. Tectonophysics 352, 87–103.

Othman, B.D., Polve, M., Allègre, C.J., 1984. Nd–Sm–Sr isotopic composition of granulites and constraints on the evolution of the lower continental crust. Nature 307, 510.

Perejón, A., Moreno Eiris, E., Abad, A., 1994. Montículos de arqueociatos ycalcimicrobios del Cámbrico Inferior de Terraldes, Gerona (Pirineo Oriental, España). Bol. R. Soc. Hist. Nat., Secc. Geol. 89, 55–95.

Pidgeon, R.T., Furfaro, D., Kennedy, A.K., Nemchin, A.A., van Bronswijk, W., 1994. Calibration of zircon standards for the Curtin SHRIMP II. U.S. Geol. Surv. Circ. 1107, 251.

Pin, C., Marini, F., 1993. Early Ordovician continental break-up in Variscan Europe: Nd–Sr isotope and trace element evidence from bimodal igneous associations of the Southern Massif central, France. Lithos 29, 177–196.

Rodríguez-Alonso, M.D., Peinado, M., López-Plaza, M., Franco, P., Carnicero, A., Gonzalo, J.C., 2004. Neoproterozoic–Cambrian synsedimentarymagmatism in the Centrallberian Zone (Spain): geology, petrology and geodynamic significance. Int. J. Earth Sci. 93, 897–920.

Roger, F., Respaut, J.P., Brunel, M., Matte, Ph., Paquette, J.L., 2004. Première datation U–Pb des orthogneiss oeillés de la zone axiale de la Montgane Noire (Sud du Massif central): nouveaux témoins du magmatisme ordovicien dans la chaîne varisque. C. R. Geosci. 336,19–28.

Samson, S.D., D'Lemos, R.S., Miller, B.V., Hamilton, M.A., 2005. Neoproterozoic palaeogeography of the Cadomia and Avalon terranes: constraints from detrital zircon U–Pb ages. J. Geol. Soc. Lond. 162, 65–71.

Santanach, P.F., 1972a. Estudio tectónico del Paleozoico inferior del Pirineo entre la Cerdaña y el río Ter. Acta Geol. Hisp. 7, 44–49.

Santanach, P.F., 1972b. Sobre una discordancia en el Paleozoico inferior de los Pirineos orientales. Acta Geol. Hisp. 7, 129–132.

Santos Zalduegui, J.F., Schärer, U., Gil Ibarguchi, J.I., 1995. Isotope constraints on the age and origin of magmatism and metamorphism in the Malpica–Tuy allochthon, Galicia, NW Spain. Chem. Geol. 121, 91–103.

Silva, J.B., Pereira, M.F., 2004. Transcurrent continental tectonics model for the Ossa–MorenaZone Neoproterozoic–Paleozoic evolution, SW Iberian Massif, Portugal. Int. J. Earth Sci. 93, 886–896.

Simancas, F., Expósito, I., Azor, A., Martínez Poyatos, D., González Lodeiro, F., 2004. From the Cadomian orogenesis to the Early Paleozoic Variscan rifting in Southwest Iberia. J. Iber. Geol. 30, 53–71.

Stacey, J.S., Kramers, J.D., 1975. Approximation of terrestrial lead isotope evolution by a two-stage model. Eart Planet. Sci. Lett. 26, 207–221.

Stampfli, G.M., von Raumer, J.F., Borel, G.D., 2002. Paleozoic evolution of pre-Variscan terranes: From Gondwana to the Variscan collision. In: Martínez Catalán, J.R., Hatcher, R.D., Arenas, R., Díaz García, F. (Eds.), Variscan-Appalachian dynamics: The building of the late Paleozoic basement. Boulder, Colorado. Geol. Soc. Am. Special Paper, vol. 364, pp. 263–280.

Valladares, M.I., Ugidos, J.M., Barba, P., Colmenero, J.R., 2002. Contrasting geochemical features of the Central Iberian Zone shales (Iberian Massif, Spain): implications for the evolution of Neoproterozoic–Lower Cambrian sediments and their sources in other peri-Gondwanan areas. Tectonophysics 352, 121–132.

Valverde-Vaquero, P., Dunning, G.R., 2000. New U–Pb ages for Early Ordovician magmatism in Central Spain. J. Geol. Soc. Lond. 157, 15–26.

Vitrac-Michard, A., Allègre, C.J., 1975. ^{238}U–^{206}Pb, ^{235}U–^{207}Pb, systematics on Pyrenean basement. Contrib. Mineral. Petrol. 51, 205–212.

von Raumer, J., Stampfli, G.M., 2008. The birth of the Rheic Ocean – Early Palaeozoic subsidence patterns and subsequent tectonic plate scenarios. Tectonophysics. 461, 9–20 (this issue). doi:10.1016/j.tecto.2008.04.012.

von Raumer, J.F., Stampfli, G.M., Borel, G., Busy, F., 2002. Organization of pre-Variscan basement areas at the north-Gondwanan margin. Int. J. Earth Sci. 91, 35–52.

Williams, I.S., 1998. U–Th–Pb geochronology by ion-microprobe. In: McKibben, M., Shanks, W., Ridley, W. (Eds.), Applications of Microanalytical Techniques to Understanding Mineralizing Process. Rev. Econ. Geol., vol. 7, pp. 1–35.

Williams, I.S., Hergt, J.M., 2000. U–Pb dating of Tasmanian dolerites: a cautionary tale of SHRIMP analysis of high-U zircon. In: Woodhead, J.D., Hergt, J.M., Noble, W.P. (Eds.), Beyond 2000: New frontiers in isotope geoscience, Lorne, 2000, pp. 185–188. Abstracts and Proceedings.

Zwart, H.J., 1979. The geology of the Central Pyrenees. Leidse Geol. Meded. 50, 1–74.